Proceedings of the
44th IEEE Conference on Decision and Control, and
the European Control Conference 2005
Seville, Spain, December 12-15, 2005



# Trajectory Tracking of a Piezoelectric System using State Compensated Iterative Learning Control

Chiang-Ju Chien, Fu-Shin Lee, and Jhen-Cheng Wang

*Abstract*—**This paper proposes a novel scheme of state compensated iterative learning control (ILC) for trajectory tracking of piezoelectric systems. The new ILC scheme adds a state compensation term to the conventional Arimoto-type ILC formula. The state compensation term is based on the difference of tracking error between the current and previous iterations. With the aid of this state compensation, iterative learning control can therefore take effect more precisely as desired. Further, the addition of the current error in the compensation term can also serve the role of feedback control to stabilize the system. The new ILC scheme keeps the simplicity feature of conventional iterative learning control that no model is required for control purpose. Experimental results demonstrate that a piezoelectric actuator using the proposed learning scheme can achieve error convergence in about three to five iterations, and keep steady-state tracking errors reaching the system noise level.**

## I. Introduction

Piezoelectric actuators have been widely used for precision positioning in various engineering fields, such as positioning of masks in microelectronics, positioning of mirrors or lenses in optics, and positioning of diamond tools in mechanical engineering. A piezoelectric actuator is made of ferroelectric ceramic materials, typically lead, zirconate and titanate (PZT) compounds. Driven by a dipole electrical field, the crystal structure of the PZT material is polarized and deformed, which results in the excited displacement of the PZT actuator. After removal of the applied electric field, however, residual polarization or displacement remains within the material. Under cyclic driving, the piezoelectric actuator therefore exhibits nonlinear relations between the input voltage and the output displacement, which is the well-known hysteresis loop.

The nonlinear phenomena of piezoelectric actuators have attracted a lot of research over the past years. Various control schemes have been proposed to compensate for the nonlinear behaviors of piezoelectric systems. Many schemes were inversion based by using inversions of certain hysteresis models, e.g. the notable Preisach model, in the feed-forward path [1], and/or the PID control or the like in the feedback path [2]. More complex control methods such as H-infinity, neural sliding-mode control, etc. were also reported [3]-[4]. All such endeavors have attempted to reduce tracking errors of piezoelectric systems to about 1~5% of stroke lengths.

Some studies changed their strategies to other easier approaches such as the iterative learning control (ILC), which is simple and requires no models for controlling repetitive tasks. The ILC theory has been developed for decades and also been applied to various tasks that are repetitive in nature [5]. A few ILC applications in the literature are relevant to our research of piezoelectric actuator tracking, and are briefed as follows. In [6], the basic p-type ILC was used for piezoactuator tracking. Its tracking performance for a slow monotonic trajectory was excellent, though the tracking of a sinusoidal trajectory seemed less impressive. In [7], the basic p-type ILC was applied to track noise disturbed trajectories for a piezoelectric stage under PID control. It further introduced a disturbance observer to improve tracking accuracy. In [8], a current error assisted ILC scheme was used for position tracking of a piezoelectric motor. It improved tracking errors drastically, compared to a traditional PI controller. In [9], the current authors proposed a model-based ILC algorithm that learns the model error iteratively. The model-based ILC achieved good performance on piezoactuator tracking, but it requires a model of the system for tracking control.

In this study, we propose a state compensated iterative learning control (SCILC) scheme for trajectory tracking of piezoelectric actuators. The conventional ILC theory is based on some assumptions such as the identical initial condition and the Lipschitz condition. In practice of tracking nonlinear systems such as piezoelectric actuators, however, initial conditions on different iterations may vary substantially, and the Lipschitz condition may not be satisfied either. The conventional ILC may thus not succeed in tracking control as expected. For this regard, we introduce the concept of using state compensation to modify the conventional ILC. With this state compensation, the conventional ILC can offset the state difference between the current and previous iterations all the time, and therefore learn from the previous iteration as desired. Furthermore, this state compensation depends only on tracking errors of the two iterations; no system model is required.

In addition to the proposal of an ILC algorithm, an

Manuscript submitted Sep. 10, 2005. This work was supported by the National Science Council, R.O.C., under Grant NSC93-2218-E-211-002 and NSC93-2212-E-211-007.

Chiang-Ju Chien is with the Department of Electronic Engineering, Huafan University, Shihtin, Taipei 223 Taiwan, Republic of China. (Correspondence phone: 886-2-26632102 ext. 4120; fax: 886-2-86606675; e-mail: cjc@huafan.hfu.edu.tw).

Fu-Shin Lee is with the Department of Mechatronic Engineering, Huafan University, Shihtin, Taipei 223 Taiwan, Republic of China. (e-mail: fslee@ huafan.hfu.edu.tw).

Jhen-Cheng Wang is with the Department of Electronic Engineering, Tungnan Inst. of Tech., Shenkeng, Taipei 222 Taiwan, Republic of China. (e-mail: jcwang@mail.tnit.edu.tw).

0-7803-9568-9/05/$20.00 ©2005 IEEE

important issue is filtering of tracking errors. In practice of ILC, it is typical to filter the error data acquired during the previous iteration, so that good transients and learning robustness can be achieved [10]. This error filtering is especially important when iterative errors approach the system noise level. In this situation, if there is no proper error filtering, ILC might be learning or amplifying system noises rather than error signals. Longman [11] maintains that long term stability is a serious issue in iterative learning control and suggests using zero-phase filtering as one treatment in this regard. Hence, the design of zero-phase filtering is included in this study.

Another important issue is convergence analysis of the proposed ILC algorithm. We can approach it in frequency domain, and thus derive a formula for the convergence bandwidth. Theoretically, the cutoff frequency of zero-phase filtering should fall within the convergence bandwidth, so that tracking errors can converge monotonically for all frequencies below cutoff. On the other hand, the cutoff frequency can be selected to cover significant signal spectra of tracking errors rather than noises, so that significant error signals instead of noises can be learned by ILC. For nonstationary tracking errors, a time-frequency analysis (TFA) of errors can be adopted in this regard.

The following paper consists of major sections covering the proposed SCILC theory, the error filtering issue, convergent analysis, time-frequency analysis of tracking errors, and an experiment.

## II. State Compensated ILC

Piezoelectric actuator systems are nonlinear and can be characterized by substantial hysteresis behaviors. Applying ILC to tracking control of piezoelectric actuators is attractive since it requires no complicated model of a piezoelectric actuator system. In this section, we review briefly the basic Arimoto-type ILC, a typical current error assisted ILC, and then introduce the novel state compensated ILC.

In discrete-time, the basic Arimoto-type ILC has the formula

$$u_i(n) = u_{i-1}(n) + L\, e_{i-1}(n+1) \tag{1}$$

and the current error assisted ILC has a typical formula [8]

$$u_i(n) = u_{i-1}(n) + L\, e_{i-1}(n+1) + K_p e_i(n) \tag{2}$$

In the above formulae, $u$ is the input command, $e$ is the output error between the desired and measured output, $L$ is the learning gain, $K_p$ is the proportional gain, $n$ is the time step, and the subscripts $i$ and $i-1$ are iteration indexes for the current iteration and the previous iteration, respectively. In theory, error convergence of conventional ILC for nonlinear systems can be proved by assuming certain conditions. In practice of ILC, however, these assumptions may not be satisfied on all iterations, and thus experiments may not yield desired results.

To solve this problem, we propose a state compensated ILC scheme by adding a state compensation term to the Arimoto-type ILC. This state compensated ILC has the update formula:

$$u_i(n) = u_{i-1}(n) + L\, e_{i-1}(n+1) + K\left[e_i(n) - e_{i-1}(n)\right] \tag{3}$$

where $K$ is the compensation gain. The $K$-term , i.e. $K\left[e_i(n) - e_{i-1}(n)\right]$, is designed to offset the state difference between the current and previous iterations at any time $n$. With this state compensation, the Arimoto-type ILC can therefore control tracking of piezoelectric actuators more precisely. The SCILC compensates for state difference all the time, and is thus not restricted by assumptions imposing on conventional ILC for error convergence. Moreover, the current error $e_i(n)$ in the $K$-term can also function as feedback control to stabilize the system. It is similar to the role of the current error $e_i(n)$ in (2).

## III. Filtering of Tracking Errors

In the above ILC formulae (1), (2) , and (3), the learnable error term is $e_{i-1}(n+1)$ which is the error output caused by the input $u_{i-1}(n)$ in the previous iteration. This error term is naturally contaminated by input and output disturbances in a real system, and should be filtered before ILC learns it in the current iteration. Let $\tilde{e}_{i-1}(n+1)$ denote the filtered output of $e_{i-1}(n+1)$ . Then we have the ILC implementation equations

$$u_i(n) = u_{i-1}(n) + L\, \tilde{e}_{i-1}(n+1), \tag{4}$$

$$u_i(n) = u_{i-1}(n) + L\, \tilde{e}_{i-1}(n+1) + K_p e_i(n), \tag{5}$$

and $$u_i(n) = u_{i-1}(n) + L\, \tilde{e}_{i-1}(n+1) + K\left[e_i(n) - e_{i-1}(n)\right], \tag{6}$$

for the Arimoto-type ILC, the current error ILC, and the SCILC, respectively. In (5), we do not filter the current error $e_i(n)$, since such filtering will cause certain phase delay to the current error, which is not desirable. Similarly in (6), $e_i(n)$ is not filtered, and thus neither its counterpart $e_{i-1}(n)$.

Filtering $e_{i-1}(n+1)$ with no phase delay, i.e. zero-phase filtering, is briefed as follows. In this paper, let $F$, $\Omega$, $f$, and $\omega$ denote the analog frequency (Hz), the analog radian frequency (rad/sec), the digital frequency (cycle/sample), and the digital radian frequency (rad/sample), respectively. An ideal linear-phase filter with a desired cutoff frequency $\omega_c$ and a phase delay of $(N-1)/2$ can be shown to have an impulse response [12]

$$h_d(n) = \frac{\sin\left(n - \frac{N-1}{2}\right)\omega_c}{\pi\left(n - \frac{N-1}{2}\right)}, \quad -\infty < n < \infty$$

By using a window such as the Hamming window to truncate the ideal $h_d(n)$, one can implement the linear-phase filtering on a practical filter of a length $N$ that has an impulse

response as

$$h(n)=\left(0.54-0.46\cos\frac{2\pi n}{N-1}\right)\frac{\sin(n-\frac{N-1}{2})\omega_c}{\pi(n-\frac{N-1}{2})} \tag{7}$$

where $n\in[0,N-1]$. Zero-phase filtering of $e_{i-1}(n+1)$ can be then realized using

$$\tilde{e}_{i-1}(n+1)=h(n)*e_{i-1}(n+1+\frac{N-1}{2}) \tag{8}$$

where the notation * means convolution and the filter length $N$ is assumed an odd length.

## IV. Convergence Analysis of SCILC

Convergence analysis of the SCILC based on its implementation equation (6) can be approached in frequency domain. First, by inserting (8) into (6), one obtains

$$\begin{aligned}u_i(n)= \;& u_{i-1}(n)+K\left[e_i(n)-e_{i-1}(n)\right]\\ &+Lh(n)*e_{i-1}(n+1+\frac{N-1}{2})\end{aligned} \tag{9}$$

Performing z-transform of (9) leads to

$$\begin{aligned}U_i(z)= \;& U_{i-1}(z)+K\left[E_i(z)-E_{i-1}(z)\right]\\ &+LH(z)z^{1+(N-1)/2}E_{i-1}(z)\end{aligned} \tag{10}$$

Evaluating (10) on the unit circle $z=e^{j2\pi f}$ gives rise to the frequency domain expression

$$\begin{aligned}U_i(f)= \;& U_{i-1}(f)+K\left[E_i(f)-E_{i-1}(f)\right]\\ &+LH(f)e^{j2\pi f[1+(N-1)/2]}E_{i-1}(f)\end{aligned} \tag{11}$$

Here, the frequency response of a linear-phase filter such as (7) can be shown as

$$\begin{aligned}H(f)= \;& e^{-j2\pi f(N-1)/2}\times\left\{h\left(\frac{N-1}{2}\right)\right.\\ &\left.+\sum_{n=0}^{(N-3)/2}2h(n)\cos 2\pi f\left(\frac{N-1}{2}-n\right)\right\}\end{aligned} \tag{12}$$

where $f=\omega/2\pi$. Then, substituting (12) into (11) gives

$$\begin{aligned}U_i(f)= \;& U_{i-1}(f)+K\left[E_i(f)-E_{i-1}(f)\right]\\ &+Le^{j2\pi f}E_{i-1}(f)\times\left\{h\left(\frac{N-1}{2}\right)\right.\\ &\left.+\sum_{n=0}^{(N-3)/2}2h(n)\cos 2\pi f\left(\frac{N-1}{2}-n\right)\right\}\end{aligned} \tag{13}$$

Rearranging (13) yields

$$U_i(f)=U_{i-1}(f)+G_{ff}(f)E_{i-1}(f)+G_{fb}E_i(f) \tag{14}$$

where

$$G_{fb}=K \tag{15}$$

$$\begin{aligned}G_{ff}(f)= \;& -K+Le^{j2\pi f}\left\{h\left(\frac{N-1}{2}\right)\right.\\ &\left.+\sum_{n=0}^{(N-3)/2}2h(n)\cos 2\pi f\left(\frac{N-1}{2}-n\right)\right\}\end{aligned} \tag{16}$$

Since the linear-phase filter in our design is symmetric, i.e. $h(n)=h(N-1-n)$, one can rewrite (16) as

$$\begin{aligned}G_{ff}(f)= \;& -K+Le^{j2\pi f}\\ &\times\sum_{n=0}^{N-1}h(n)\cos 2\pi f\left(\frac{N-1}{2}-n\right)\end{aligned} \tag{17}$$

Now, by assuming the plant is linear and has a transfer function $G_p(f)$, the output $Y_i(f)$ in iteration $i$ is

$$Y_i(f)=G_p(f)U_i(f) \tag{18}$$

Hence

$$E_i(f) = Y_d(f)-G_p(f)U_i(f) \tag{19}$$

where $E_i(f)$ is the error and $Y_d(f)$ is the desired output. Similarly, for the previous iteration $i-1$,

$$E_{i-1}(f) = Y_d(f)-G_p(f)U_{i-1}(f) \tag{20}$$

Then, inserting (14) into (19) leads to

$$\begin{aligned}E_i(f)= \;& \left[Y_d(f)-G_p(f)U_{i-1}(f)\right]\\ &-G_p(f)\times\left[G_{ff}(f)E_{i-1}(f)+G_{fb}E_i(f)\right]\end{aligned} \tag{21}$$

Substituting (20) into (21) reduces to

$$\begin{aligned}E_i(f)= \;& E_{i-1}(f)-G_p(f)\\ &\times\left[G_{ff}(f)E_{i-1}(f)+G_{fb}E_i(f)\right]\end{aligned} \tag{22}$$

Rearranging (22) produces

$$\frac{E_i(f)}{E_{i-1}(f)}=\frac{1-G_{ff}(f)G_p(f)}{1+G_{fb}G_p(f)} \tag{23}$$

Ideally, learning errors will delay monotonically if

$$\left|\frac{1-G_{ff}(f)G_p(f)}{1+G_{fb}G_p(f)}\right|<1 \quad ,\forall f \tag{24}$$

By substituting (15) and (17) into (24), one obtains the convergence criterion:

$$|A(f)|<1 \quad ,\forall f \tag{25}$$

where

$$A(f)=1-\frac{LG_p(f)e^{j2\pi f}\sum_{n=0}^{N-1}h(n)\cos 2\pi f\left(\frac{N-1}{2}-n\right)}{1+KG_p(f)} \tag{26}$$

is the convergence argument.

In many situations, however, (25) may not hold for all frequencies. Instead, the inequality may be valid only for frequencies below certain threshold. Hence, we define a convergence bandwidth $f_b$ as the threshold frequency that satisfies

$$|A(f_b)|=1 \tag{27}$$

If (27) has multiple real roots, then $f_b$ is the minimal positive root; if (27) has no real root, $f_b$ is assigned as the Nyquist frequency. It is obvious that one should pick up a filter cutoff frequency that satisfies the inequality condition

$$f_c<f_b \tag{28}$$

for error convergence.

## V. TIME-FREQUENCY ANALYSIS OF TRACKING ERRORS

Convergence analysis of the SCILC imposes the convergence bandwidth as the upper bound of the cutoff frequency for filtering. In practice of ILC, we can select a cutoff frequency somewhere below the upper bound, such that the signal part of tracking errors is kept whereas the noise part is filtered out. Distinguishing the signal part from the noise part can be accomplished by analysis of tracking errors. To analyze nonstationary data such as tracking errors, representative methods are Short-Time Fourier Transform (STFT), Wavelet Transform (WT), and Wigner-Ville Distribution (WVD). In general, the WVD can characterize time-dependent spectra of the data better than STFT and WT [13], but it has the drawback of cross-term interference. Nevertheless, the interference problem can be treated by WVD variations, such as the notable smoothed pseudo WVD [13]. Referring to ILC studies using time-frequency analysis such as [14], we adopt the WVD for analysis of tracking errors. Three basic properties of the WVD are as follows.

The WVD of a signal $x(t)$ is defined as

$$W_x(t,F)=\int_{-\infty}^{\infty} x(t+\frac{\tau}{2})x^*(t-\frac{\tau}{2})e^{-j2\pi F\tau}d\tau \tag{29}$$

From $W_x(t,F)$, the instantaneous frequency (IF) of $x(t)$ can be recovered as

$$F_x(t)=\frac{\int_{-\infty}^{\infty} W_x(t,F)FdF}{\int_{-\infty}^{\infty} W_x(t,F)dF} \tag{30}$$

Due to the frequency marginal property of the WVD, the energy density spectrum (EDS) of $x(t)$ can be obtained by

$$\left|X(F)\right|^2=\int_{-\infty}^{\infty} W_x(t,F)dt \tag{31}$$

Computation of the WVD for discrete-time signals can be made with the aid of TFA toolboxes such as [15].

## VI. EXPERIMENT OF SCILC

The experiment platform includes a piezoelectric system, a data acquisition card, and a personal computer. The piezoelectric system consists of a power amplifier (input $-1$v to $+5$v, amplification 30), a piezoelectric actuator with a built-in strain gauge (input $-30$v to $+150$v, output $-8\mu m$ to $40\mu m$), and a sensor circuit (sensor output $+0.2$v to $-1$v). The data acquisition card has 12-bit A/D and D/A converters (sampling rate 100kS/s maximum for input and 1kS/s maximum for output).

The major control task was tracking of a sinusoidal trajectory with a frequency 10Hz and a stroke length $32\mu m$. The desired sinusoidal trajectory had total 50 samples with a sampling rate of 500 samples per second, and was tracked for five cycles per iteration. Besides the initial iteration, there were total 100 learning iterations. Here, the ILC controller was designed as follows.

### A. Iterative Learning Controller Design

*1) Learning Gain and Compensation Gain*

To simplify our experiments, we decided to assign the compensation gain $K$ a value equal to the learning gain $L$, i.e. $K=L$. We calculated the nominal feed-forward gain $g$ of the system, which was $-1/5$ due to the conversion from the power amplifier input of +5v maximum to the sensor output of $-1$v maximum. We then took $g^{-1}$, i.e. $-5$, as the value for both the learning gain and the compensation gain in the experiments.

*2) Convergence Bandwidth*

One can plot the frequency response of the convergence argument $A(f)$ according to (26), if $L$, $K$, $G_p(f)$, $N$, and $h(n)$ are all known. In the previous subsection, both $L$ and $K$ were assigned as $-5$. Further, as described in the following two subsections, the filter length $N$ and the cutoff frequency $f_c$ will be designed as 35 and 0.15, respectively. The filter impulse response $h(n)$ can be thus derived. Therefore, once the frequency response of plant $G_p(f)$ is known, the Bode plot of $A(f)$ can be obtained.

In Fig. 1-a, we show two Bode plots of $A(f)$. One plot is based on $G_p(f)$ equal to the nominal feed-forward gain $g$, i.e. $-1/5$. The other plot is based on a rough estimation of the system transfer function [9]

$$\hat{G}_p(f)=\frac{-0.0823e^{-\mathrm{j}2\pi f}-0.0068e^{-\mathrm{j}4\pi f}+0.0564e^{-\mathrm{j}6\pi f}}{1-0.873e^{-\mathrm{j}2\pi f}} \tag{32}$$

One can observe from Fig. 1-b, which is a zoom-in plot of Fig. 1-a, that the convergence bandwidth is about 0.2:

$$f_b\approx 0.2 \tag{33}$$

no matter $G_p(f)$ equals $g$ or $\hat{G}_p(f)$.

*3) Filter Length*

In general, the FIR filter has an inverse relationship between the filter length and the transition bandwidth: the longer the filter, the narrower the transition, or vice versa. An empirical formula between them, for a Hamming window based FIR filter, is given by [16]

$$N\approx\frac{3.47}{f_t} \tag{34}$$

where $f_t$ is the width of the transition band. Here, we chose a simple value 0.1 as the transition bandwidth, i.e.

$$f_t=0.1 \tag{35}$$

Hence by inserting Equation (35) into Equation (34), one obtains a reasonable filter length

$$N\approx 35 \tag{36}$$

*4) Cutoff Frequency*

To determine the cutoff frequency of zero-phase filtering, different approaches were proposed. For example, [17]

adopted the −3dB frequency of the desired system function as the cutoff frequency, whereas [18] proposed a scheme of iteration-varying and time-varying cutoff frequencies up to the convergence bandwidth under a phase lead learning control. In our design, we determined the cutoff frequency by using both time-frequency analysis and convergence bandwidth analysis of tracking errors, as follows.

Applying the WVD equations (29)-(31) and the smoothed pseudo WVD variation to tracking errors under different control regemes [9], we obtained figures on WVDs, and IF and EDS estimations of tracking errors. Fig. 2 is a typical figure that depicts the smoothed pseudo WVD analysis results of tracking errors during a learning iteration. From Fig. 2, one can observe that tracking errors have major frequency components located in two separate bands: a lower-frequency band below a frequency of about 0.1, and a higher-frequency band above a frequency of roughly 0.15. We can reasonably assume that lower-band errors were correlated to input signals, while higher-band errors were caused by system disturbances.

Judging from the convergence bandwidth equation (33) and the WVD analysis above, we chose, for simplicity, 0.1 as the edge frequency of the filter passband. This implies an edge frequency of the stopband at 0.2 since the transition bandwidth is 0.1 (35). Following the convention in the signal processing toolbox of MATLAB, the cutoff frequency of the Hamming windowed FIR filter is defined as the −6dB frequency, and thus

$$f_c = 0.15 \tag{37}$$

This result satisfies the inequality (28) for error convergence.

### B. Experimental Results

Fig. 3-a plots typical RMS errors of total 100 SCILC iterations. From Fig. 3-a, one can observe that tracking errors converge within about 3~5 iterations and the converged RMS errors are around 0.25% of the actuator stroke length. In contrast, tracking experiments using conventional ILC, i.e. the Arimoto-type ILC formula (4) and the current error assisted ILC formula (5), have typical errors shown by Fig. 3-b. The solid line in Fig. 3-b indicates that steady-state tracking errors of the Arimoto-type ILC vary considerably around a mean value of about RMS 0.5% of the stroke length. Moreover, as shown by the broken line in Fig. 3-b, the current error assisted ILC using $K_p = -5$ has a tracking error curve that first converges in a couple of iterations and then diverges abruptly. By comparing Fig. 3-a with Fig. 3-b, it is obvious that the new state compensated ILC scheme outperforms conventional ILC substantially.

It is reasonable to estimate the root-mean-square value of system uncertainties to be about 0.2%, as considering the strain gauge accuracy and the ADC and DAC accuracies. Therefore, we conclude that, on trajectory tracking of the piezoelectric system, our proposed control scheme is effective for achieving fast error convergence in several iterations as well as for keeping long-term stability of tracking errors close to the background noise level.

Fig. 3-a is a typical experimental result based on the ILC controller parameters $L$, $K$, $f_c$, and $N$ equal to the design values of $-5$, $-5$, 0.15, and 35, respectively. In experiments using different parameter values, we could still obtain similar results for tolerances of these parameters being at least $\pm 2$, $\pm 2$, $\pm 0.05$, and $\pm 20$, respectively. This means that the proposed ILC controller is quite robust in terms of controller parameter variations.

## VII. CONCLUSION

A novel state compensated ILC scheme successfully carries out trajectory tracking of a piezoelectric system. It achieves fast learning transition in about three to five iterations, and keeps long term stability of tracking errors reaching the system noise level. Besides learning the learnable error as the conventional ILC does, this state compensated ILC employs the difference of tracking error between the current and previous iterations to compensate for the difference of state between the two iterations at any time. The scheme adopts an FIR filter for attaining zero-phase low-pass filtering of tracking errors. The cutoff frequency of the filter is decided by using both the WVD time-frequency analysis and the convergence bandwidth analysis of tracking errors. Future work will focus on high-order ILC to further enhance noise immunity on tracking control.

## REFERENCES


[1] P. Ge and M. Jouaneh, "Tracking control of a piezoceramic actuator," *IEEE Transactions on Control Systems Technology*, vol. 4, pp. 209–216, 1996.

[2] J. Tzen, S. Jeng, and W. Chieng, "Modeling of piezoelectric actuator for compensation and controller design," *Precision Engineering*, vol. 27, pp. 70–86, 2003.

[3] S. Salapaka, A. Sebastian, J.P. Cleveland, and M.V. Salapaka, "Design, identification and control of a fast nanopositioning device," *Proceedings of the 2002 American Control Conference*, vol.3, pp. 1966–1971, 2002.

[4] C.L. Hwang and C. Jan, "A reinforcement discrete neuro-adaptive control for unknown piezoelectric actuator systems with dominant hysteresis," *IEEE Transactions on Neural networks,* vol. 14, no. 1, pp. 66–78, 2003.

[5] Z. Bien and J.X. Xu, *Iterative Learning Control - Analysis, Design Integration and Application*, Norwell, MA: Kluwer Academic Publishers, 1998.

[6] K. Leang and S. Devasia, "Iterative feedforward compensation of hysteresis in piezo positioners," *Proceedings of the 2003 IEEE Conference on Decision and Control,* vol. 3, pp. 2626–2631, 2003.

[7] Y.C. Huang and C.H. Cheng, "Robust tracking control of a novel piezodriven monolithic flexure-hinge stage," *Proc. of*

*the 2004 IEEE Conference on Control Applications*, pp. 977–982, 2004.

[8] J.X. Xu, J. Xu, and T. Lee, "Iterative learning control for a linear piezoelectric motor with a nonlinear unknown input deadzone," *Proc. of the 2004 IEEE Conference on Control Applications*, pp. 1001–1006, 2004.

[9] C.J. Chien, F.S. Lee, J.C. Wang, and P.J. Chen, "Application of iterative learning to tracking control of a piezoelectric system," *Proc. of the 2004 IEEE Conference on Control Applications*, pp. 376–381, 2004.

[10] H. Elci, R. Longman, M. Phan, J. Juang, and R. Ugoletti, "Simple learning control made practical by zero-phase filtering: applications to robotics," *IEEE Transactions on Circuits and Systems I: Fundamental Theory and Applications,* vol. 49, no.6, pp. 753–767, 2002.

[11] R. Longman, "Practical design of learning and repetitive control," *Workshop Tutorial on Learning Control Design and Applications*, *the 2004 IEEE Conference on Control Applications*, Taipei, Taiwan, pp. 33–125, 2004.

[12] J. Proakis and D. Manolakis, *Digital signal processing: principles, algorithms, and applications*, Upper Saddle River, NJ: PTR Prentice Hall, 1996.

[13] S. Qian and D. Chen, *Joint time-frequency analysis: methods and applications*. Upper Saddle River, NJ: Prentice Hall, 1996.

[14] Y. Chen and K. Moore, "Frequency domain adaptive learning feedforward control," *Proceedings of the 2001 IEEE International Symposium on Computational Intelligence in Robotics and Automation*, pp. 396–401, 2001.

[15] F. Auger, P. Flandrin, O. Lemoine, and P. Goncalves, Time-frequency toolbox for Matlab: Tutorial. http://iut-saint-nazaire.univ-nantes.fr /~auger/tftb.html, 1999.

[16] A. Ambardar, *Analog and digital signal processing*, 2nd ed., Pacific Grove, CA: Brooks/Cole Pub. Co., 1996.

[17] K.K. Tan, H. Dou, and Y. Chen, "High precision linear motor control via relay-tuning and iterative learning based on zero-phase filtering," *IEEE Transactions on Control Systems Technology*, vol. 9, no. 2, pp. 244–253, 2001.

[18] B. Zhang, D. Wang, and Y. Ye, "Wavelet transform based frequency tuning ILC," *IEEE Transactions on System, Man, and Cybernetics- Part B*, vol. 35, no. 1, pp. 107–114, 2005.

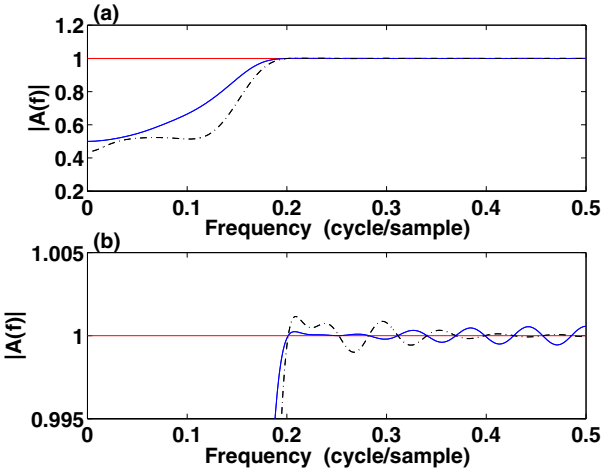


Fig. 1. Convergence argument: plots of the convergence argument magnitude $|A(f)|$ vs. frequency, in (a) full-scale view and (b) zoom-in view, for $G_p(f)$ equal to $g$ (the solid curve) and $G_p(f)$ equal to $\hat{G}_p$ (the broken curve), respectively.

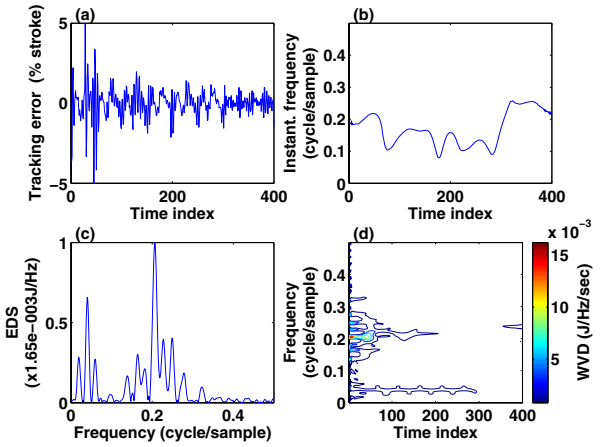


Fig. 2. The WVD analysis of tracking errors in a learning iteration: (a) a record of error measurement, (b) an estimation of the instantaneous frequency, (c) an estimation of the energy density spectrum, and (d) the smoothed pseudo Wigner-Ville Distribution.

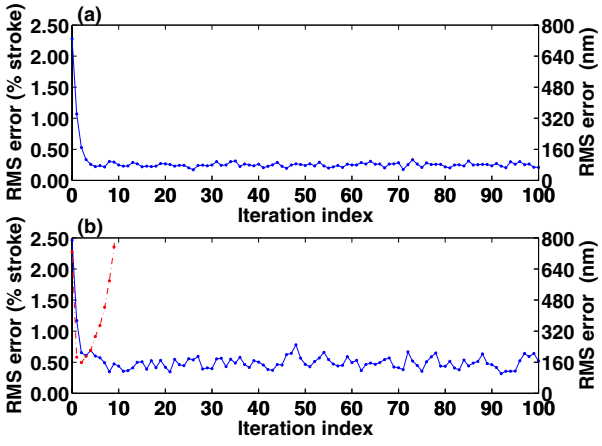


Fig. 3. Root-mean-square tracking errors vs. iteration index for total 100 iterations: (a) using the SCILC, and (b) using the Arimoto-type ILC (the solid line) and the current error assisted ILC (the broken line), respectively.